



Synthesis and Structure-Activity Relationship Studies of C(13)-Desmethylene-(-)-Zampanolide Analogs

Journal Article

Author(s):

Brütsch, Tobias M.; [Cotter, Etienne](#) ; Lucena-Agell, Daniel; Redondo-Horcajo, Mariano; Davies, Carolina; Pfeiffer, Bernhard; Pagani, Sandro; [Berardozi, Simone](#) ; Díaz, J. Fernando; Miller, John H.; Altmann, Karl-Heinz

Publication date:

2023-06-27

Permanent link:

<https://doi.org/10.3929/ethz-b-000614717>

Rights / license:

[Creative Commons Attribution-NonCommercial-NoDerivatives 4.0 International](#)

Originally published in:

Chemistry - A European Journal 29(36), <https://doi.org/10.1002/chem.202300703>

Funding acknowledgement:

149253 - Natural Products as Lead Structures for Anticancer and Antibacterial Drug Discovery: SAR Evaluation of Zampanolide and Pyridomycin (SNF)



Synthesis and Structure-Activity Relationship Studies of C(13)-Desmethylene-(–)-Zampanolide Analogs

Tobias M. Brütsch⁺,^[a, d] Etienne Cotter⁺,^[a] Daniel Lucena-Agell,^[b] Mariano Redondo-Horcajo,^[b] Carolina Davies,^[c, e] Bernhard Pfeiffer,^[a] Sandro Pagani,^[a] Simone Berardozzi,^[a, f] J. Fernando Díaz,^[b] John H. Miller,^[c] and Karl-Heinz Altmann^{*[a]}

Abstract: We describe the synthesis and biochemical and cellular profiling of five partially reduced or demethylated analogs of the marine macrolide (–)-zampanolide (ZMP). These analogs were derived from 13-desmethylene-(–)-zampanolide (DM-ZMP), which is an equally potent cancer cell growth inhibitor as ZMP. Key steps in the synthesis of all compounds were the formation of the dioxabicyclo[15.3.1]heneicosane core by an intramolecular HWE reaction (67–95% yield) and a stereoselective aza-aldol reaction with an (S)-BINOL-derived sorbamide transfer complex, to establish the C(20) stereocenter (24–71% yield). As the sole exception, for the 5-desmethyl macrocycle, ring-closure relied on macrolactonization; however, elaboration of

the macrocyclization product into the corresponding zampanolide analog was unsuccessful. All modifications led to reduced cellular activity and lowered microtubule-binding affinity compared to DM-ZMP, albeit to a different extent. For compounds incorporating the reactive enone moiety of ZMP, IC₅₀ values for cancer cell growth inhibition varied between 5 and 133 nM, compared to 1–12 nM for DM-ZMP. Reduction of the enone double bond led to a several hundred-fold loss in growth inhibition. The cellular potency of 2,3-dihydro-13-desmethylene zampanolide, as the most potent analog identified, remained within a ninefold range of that of DM-ZMP.

Introduction

Natural products represent a critical source of lead structures for drug discovery and development, and a substantial fraction of drugs approved for the treatment of human disease are either unmodified natural products or derived from a natural product lead.^[1–4] The overwhelming majority of these compounds originate from terrestrial plants, fungi or bacteria; in comparison, the impact of natural products obtained from marine organisms so far has been much less pronounced, at least partly due to their more limited availability from the natural sources.^[5,6] At the same time, many marine natural products display unique structures and bioactivities,^[7–9] which

makes them highly attractive starting points for drug discovery^[10–14] and/or valuable tools for chemical biology.^[15,16] In this context, the total chemical synthesis of marine natural products and, in particular, the chemical synthesis of analog structures is of central importance,^[17–20] as it allows to mitigate the problem of limited material supply from the producing organisms.

As a case in point, (–)-zampanolide (**1**; Figure 1) is a marine macrolide that was first isolated in 1996 by Tanaka and Higa from the marine sponge *Fasciospongia rimosa* and shown to be a potent inhibitor of cancer cell growth in vitro with IC₅₀ values in the low-nanomolar range (2–10 nM).^[21]

[a] Dr. T. M. Brütsch,⁺ E. Cotter,⁺ Dr. B. Pfeiffer, S. Pagani, Dr. S. Berardozzi, Prof. Dr. K.-H. Altmann
Department of Chemistry and Applied Biosciences
Institute of Pharmaceutical Sciences
ETH Zürich
Vladimir-Prelog-Weg 4, 8093 Zürich (Switzerland)
E-mail: karl-heinz.altmann@pharma.ethz.ch

[b] Dr. D. Lucena-Agell, Dr. M. Redondo-Horcajo, Dr. J. Fernando Díaz
Centro de Investigaciones Biológicas Margarita Salas
Consejo Superior de Investigaciones Científicas
Ramiro de Maeztu 9, 28040 Madrid (Spain)

[c] Dr. C. Davies, Prof. J. H. Miller
Centre for Biodiscovery, School of Biological Sciences
Victoria University of Wellington
6012 Wellington (New Zealand)

[d] Dr. T. M. Brütsch⁺
Current address: Dottikon Exclusive Synthesis AG
5605 Dottikon (Switzerland)

[e] Dr. C. Davies
Current address: Laboratorio de Parasitología (LAPA)
Instituto de Biología de Organismos Marinos (IBIOMAR)
(CCT CONICET-CENPAT)
Blvd. Brown 2915, Puerto Madryn (Argentina)

[f] Dr. S. Berardozzi
Current address: Syngenta AG, 4332 Stein (Switzerland)

[*] These authors contributed equally to this work.

Supporting information for this article is available on the WWW under <https://doi.org/10.1002/chem.202300703>

© 2023 The Authors. Chemistry - A European Journal published by Wiley-VCH GmbH. This is an open access article under the terms of the Creative Commons Attribution Non-Commercial NoDerivs License, which permits use and distribution in any medium, provided the original work is properly cited, the use is non-commercial and no modifications or adaptations are made.

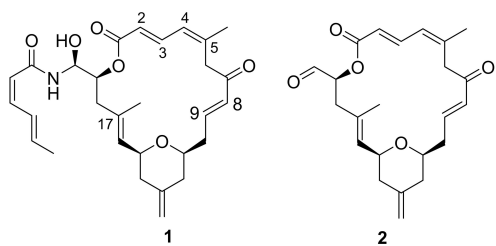


Figure 1. Structures of (–)-zampanolide (1) and (–)-dactylolide (2).

Structurally, (–)-zampanolide (1) features a dioxabicyclo[15.3.1]heneicosane core, including a polyunsaturated macrolactone ring and a *syn*-2,6-disubstituted tetrahydropyran unit bearing an exocyclic methylene group. The core is linked to a (*Z,E*)-sorbamide-derived side chain by way of a (linear) hemiaminal moiety; only few other natural products are known to incorporate this intriguing structural motif.^[22–27]

After the biology of (–)-zampanolide (1) had not been further investigated for several years after its discovery, it was re-isolated from a different sponge, *Cacospongia mycofijiensis* by Northcote and co-workers in 2009.^[28] Mode-of-action studies with the compound then revealed that 1 was a potent microtubule-stabilizing agent (MSA), thus exerting its antiproliferative effects through the same mechanism as the established anticancer drugs paclitaxel, taxotere, cabacitaxel, or ixabepilone.^[29] In contrast to the latter, however, (–)-zampanolide (1) binds to β -tubulin in a covalent fashion, as has been demonstrated by biochemical^[30] as well as structural studies.^[31] Covalent bond formation involves 1,4-addition of β -His229 to C(9) of the enone moiety in the macrocycle.^[31]

(–)-Zampanolide (1) has been the target of multiple successful total synthesis campaigns,^[32–35] including the synthesis of (+)-zampanolide (*ent*-1) by Smith and co-workers,^[36] which established the complete relative and absolute configuration of the natural product (which had not been fully elucidated by Tanaka and Higa).^[21] In addition to the total synthesis of 1, numerous synthetic studies have targeted (–)-dactylolide (2) (Figure 1),^[32–35,37] which has served as an advanced intermediate in all^[32–35] but one total synthesis of 1.^[36] This compound is significantly less potent than 1,^[35,37] thus highlighting the importance of the C(19) side chain for microtubule-stabilization and antiproliferative activity. Other aspects of the zampanolide SAR that have been investigated by means of synthetic analogs are the importance of the tetrahydropyran ring,^[35,38–42] of the C(13) methylene group^[35] and of the methyl group at C(17).^[44] Of particular importance in the context of the current study is Taylor's work on 13-desmethylene-17-desmethyl-(–)-zampanolide (5),^[44] which was found to be a 17- to 57-fold less potent cell growth inhibitor than 1 (for a 1.5:1 diastereomeric mixture at C(20); tested against 3 cancer cell lines). Unfortunately, none of the singly modified congeners (either 13-desmethylene-(–)-zampanolide (3) or 17-desmethyl-(–)-zampanolide) was reported in that study, which made it difficult to discern the effect of each of the individual modifications.

We have recently shown that the removal of the C(13) methylene group in (–)-zampanolide (1) has no discernible impact on antiproliferative activity.^[45] As the synthesis of 13-desmethylene zampanolide (3, Figure 2) includes three fewer steps than the synthesis of the parent natural product 1 (at least when employing the strategy that we have developed for the total synthesis of 1),^[35] we have based our subsequent SAR work on the 13-desmethylene macrocycle and we have used 13-desmethylene (–)-zampanolide (3) as a reference comparator to assess the effect of other modifications.

Following this approach, we have investigated the importance of the methyl groups at C(5) and C(17), of the C(2)=C(3) and C(4)=C(5) double bonds, individually and in combination, and of the enone double bond between C(8) and C(9) for microtubule-binding and antiproliferative activity.

Inspection of the structure of the complex between 1^[31] and β -tubulin shows the C(17) methyl group to be located in a hydrophobic environment, although it is unclear to what extent it actually contributes to the binding affinity of 1; in contrast, the C(5) methyl group appears not to be important for tubulin binding, but these questions needed to be addressed experimentally. Partial or complete removal of the double bonds from the conjugated system between C(1) and C(5) should provide information on the importance of conformational rigidity in this part of the structure for microtubule-binding affinity and antiproliferative activity. Finally, the removal of the C(8)=C(9) double bond in analog 9 at first glance might appear to be counterintuitive, as it is required for covalent binding to β -tubulin.^[31] However, the investigation of 9 was meant to assess the inherent binding affinity of 1 for microtubules in the absence of covalent attachment.

The corresponding analogs 5–9 (Figure 2) were all prepared via a unified global strategy. Analog 4 could not be prepared for reasons that will be discussed in detail below.

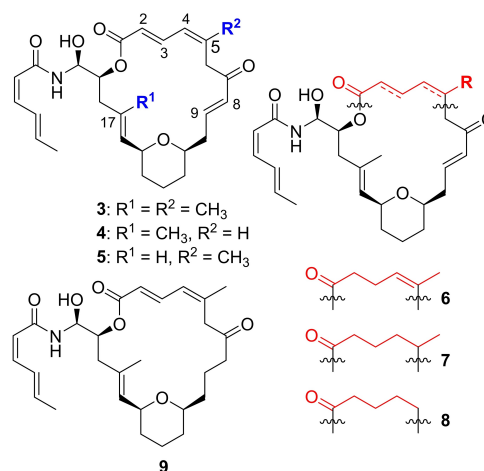
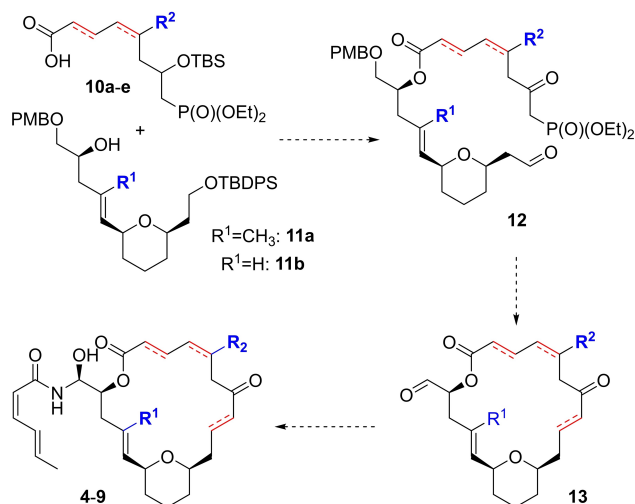


Figure 2. Structures of 13-desmethylene (–)-zampanolide (3) and of analogs targeted for SAR studies.

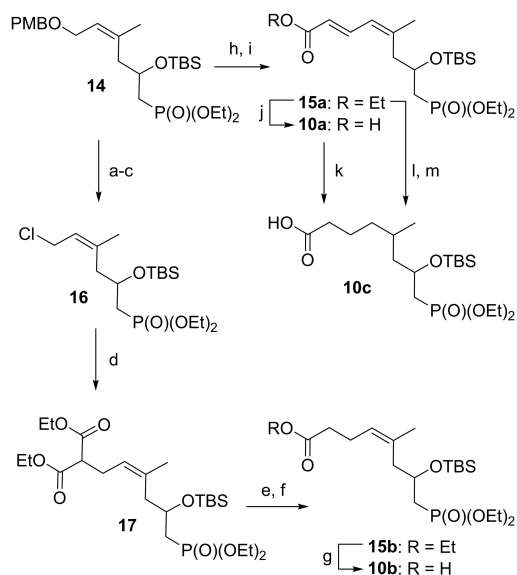
Results and Discussion

Synthetic planning

The synthesis of all analogs was to be based on our previously developed approach towards the total synthesis of (–)-zampanolide (1),^[35] which we had also followed for the synthesis of 3 and a series of morpholino-zampanolides.^[38]



Scheme 1. Global strategy for the synthesis of zampanolide analogs 4–9. Compound 10a is the precursor acid for analogs 5 and 9, 10b–d are the precursor acids for analogs 6–8, respectively, and 10e is the precursor acid for analog 4 (Figure 2).



Scheme 2. Synthesis of acids 10a–c: a) DDQ, DCM/H₂O (20:1), RT; b) DIBAL–H, DCM, –78 °C, 56% over two steps; c) MsCl, LiCl, 2,6-lutidine, 0 °C, 98%; d) Na, diethyl malonate, EtOH, reflux, 86%; e) KOH, EtOH, RT, 98%; f) Et₃N, toluene, reflux, 85%; g) 2 M NaOH, EtOH, RT, 97%; h) i) DDQ, DCM/H₂O (20:1), 0 °C; ii) (COCl)₂, DMSO, Et₃N, DCM, –78 °C to RT, 88% over two steps; j) 1 M NaOH, EtOH, 0 °C, 94% over two steps; k) H₂, 10% Pd/C, EtOH, RT, 78%; l) H₂, 10% Pd/C, EtOH, RT, 95%; m) 1 M NaOH, EtOH, 0 °C to RT, 95%.

According to this overall strategy, the ester products resulting from acylation of alcohols 11 with acids 10 would be elaborated into keto-aldehydes 12 (Scheme 1); the latter were expected to undergo *E*-selective intramolecular HWE reaction to form the corresponding macrolactones. PMB removal and oxidation would then furnish aldehydes 13, which would be reacted with (*Z,E*)-sorbamide in a stereoselective aza-aldol reaction recently developed in our laboratory,^[45] to provide analogs 4–8. Analog 9 was envisioned to be accessible from the macrocyclization product en route to 3^[35,45] by selective reduction of the enone double bond, for example by means of the Stryker reagent.

Synthesis of acids 10

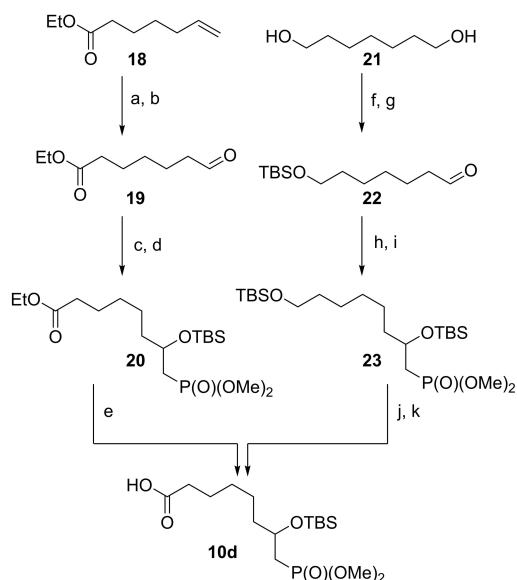
The synthesis of acid 10a via phosphonate 14 and ester 15a (Scheme 2) has been reported previously.^[35] Compound 10a was required as a precursor for the synthesis of analogs 5 and 9.

Partially saturated acid 10b was obtained from phosphonate 14,^[35] which was submitted to oxidative PMB removal with DDQ (Scheme 2). The reaction gave a mixture of the expected allylic alcohol and the corresponding aldehyde; treatment of this mixture with DIBAL–H in DCM at –78 °C yielded the desired alcohol in 56% yield over two steps. Mesylation of the primary hydroxy group followed by in situ reaction of the ensuing mesylate with LiCl then furnished allylic chloride 16 in close to quantitative yield. While attempts at the direct formation of ethyl ester 15b by alkylation of the Li-enolate of ethyl acetate (formed with LiHMDS) with 16 were unsuccessful, reaction of 16 with the Na-enolate of diethyl malonate (formed with sodium in ethanol) gave substituted malonate 17 in 86% yield after 5 min at reflux.

As Krapcho decarboxylative conditions (NaCl, DMSO/H₂O, 120–170 °C)^[46] only led to decomposition, 17 was hydrolyzed to the corresponding mono acid, which was then treated with Et₃N in toluene to induce decarboxylation. This two-step process gave ethyl ester 15b in 83% yield (from 17). Finally, saponification of 15b with NaOH/EtOH provided acid 10b in excellent yield (97%).

Fully saturated acid 10c was obtained from 10a by hydrogenation under standard conditions (H₂, 10% Pd/C, EtOH) in 78% yield as an inseparable mixture of diastereoisomers (Scheme 2). Alternatively, hydrogenation of ester 15a followed by saponification of the fully saturated product with aqueous NaOH gave 10c in 90% overall yield.

Two different approaches were elaborated towards fully saturated acid 10d (Scheme 3), which would serve as a building block for the most extensively modified zampanolide analog investigated in this study, that is, 8. Our first-generation approach towards 10d started from commercially available ethyl hept-6-enoate (18), which was converted into aldehyde 19 in 24% overall yield by hydroboration/oxidation and further oxidation of the resulting primary alcohol with pyridinium chlorochromate (PCC). Addition of lithiated dimethyl methylphosphonate to 19 at –100 °C in THF followed by TBS-protection (TBSCl, DMAP) then gave the fully protected β-



Scheme 3. Synthesis of acid **10d**: a) i: BH_3 , THF, 0°C to RT; ii: H_2O_2 , 1 M NaOH, 76% over two steps; b) PCC, DCM, 0°C to RT, 32%; c) dimethyl methylphosphonate, $n\text{BuLi}$, THF, -100°C , 35%; d) TBSCl, imidazole, DMAP, DMF, 29%; e) 1 M NaOH, EtOH, 0°C to RT, 72%; f) TBSCl, Et_3N , DCM, 0°C to RT, 54%; g) $(\text{COCl})_2$, DMSO, Et_3N , DCM, -78 to 0°C , 65%; h) dimethyl methylphosphonate, $n\text{BuLi}$, THF, -100°C ; i) TBSCl, imidazole, DMAP, DMF, 85% (two steps); j) CSA (20 mol%), DCM/MeOH (1:1), 0°C to RT, quant.; k) i: DMP, NaHCO_3 , DCM, RT; ii: NaClO_2 , NaH_2PO_4 , 2-methylbutene, $t\text{BuOH}/\text{H}_2\text{O}$, 0°C to RT, 93% (two steps).

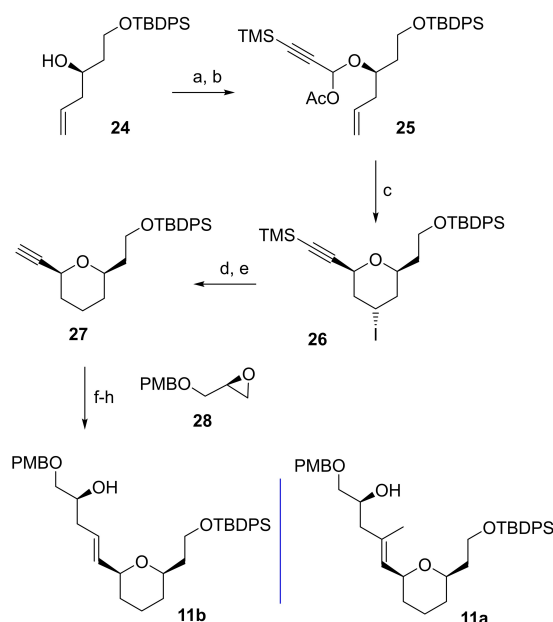
hydroxy phosphonate **20** in moderate overall yield (10%). Ester hydrolysis with aqueous NaOH finally furnished the desired acid **10d** in 72% yield. While this route would have provided sufficient amounts of analog **8** for biological testing, the poor yield for the transformation of **19** into **20** led us to seek an alternative, more efficient route towards acid **10d**.

As depicted in Scheme 3, the alternative route started with the conversion of heptane-1,7-diol (**21**) into aldehyde **22** by mono-TBS protection followed by Swern oxidation of the mono-TBS ether. While the overall yield for this transformation (35% for two steps) still leaves room for improvement, aldehyde **22** could be transformed into phosphonate **23** in 85% yield by reaction with $\text{LiCH}_2\text{P}(\text{O})(\text{OCH}_3)_2$ followed by DMAP-catalyzed silylation of the newly formed hydroxy group (vs. 10% for the conversion of **19** into **20** under the same conditions). Selective liberation of the primary hydroxy group with catalytic amounts (20 mol%) of camphorsulfonic acid in DCM/MeOH (1:1) followed by Dess–Martin oxidation^[47] of the resulting free alcohol and subsequent Pinnick oxidation^[48] of the ensuing aldehyde provided acid **10d** in excellent yield (93% over three steps). Acid **10d** could thus be obtained from heptane-1,7-diol (**21**) in six steps with an overall yield of 23%, compared to 2% for the five-step sequence from ethyl hept-7-enoate (**18**).

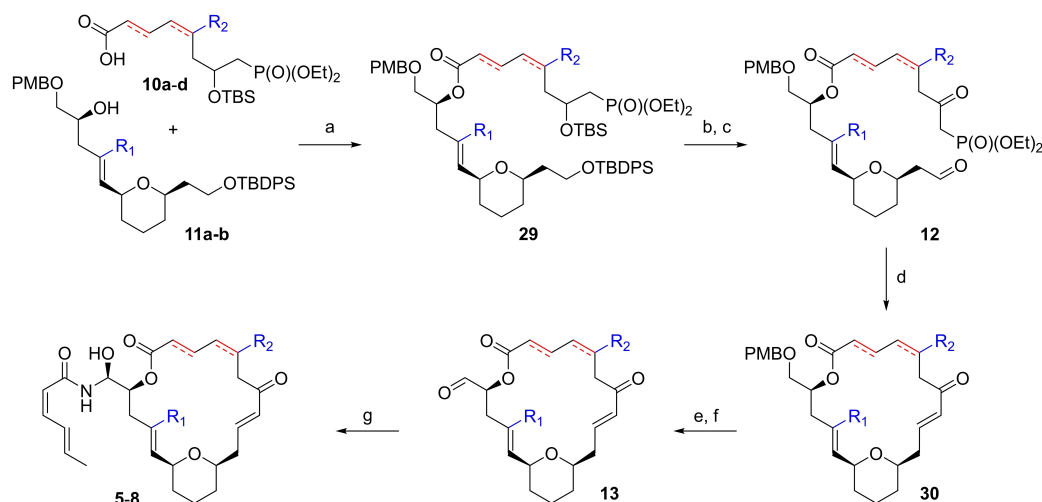
Synthesis of alcohol **11b**

The synthesis of alcohol **11b** was devised around THP-ring formation by a Prins-type cyclization as the central step (Scheme 4). The requisite cyclization precursor **25** could be obtained from homoallylic alcohol **24** by Steglich esterification with 3-TMS-propionic acid followed by DIBAL–H reduction at -78° and in situ acetylation of the ensuing hemiacetal with acetic anhydride/DMAP; **24** had also been an intermediate in the preparation of alcohol **11a**, in the context of our work on (–)-zampanolide (**1**)^[35] and 13-desmethylene(–)-zampanolide (**3**).^[45]

Somewhat surprisingly, and in contrast to our experience with the coupling of **24** and 3-butynoic acid,^[35] the esterification step proved not to be straightforward and even under optimized conditions (dropwise addition of a solution of DCC/DMAP in DCM to a solution of **24** and 3-TMS-propionic acid in DCM at -20°C) provided the desired ester **25** only in 38% yield (on a multigram scale). As a major side product, the TMS-ether of **24** was isolated in 29% yield, from which **24** could be readily recovered by treatment with aqueous HCl. While the esterification of **24** with propionic acid was slightly more efficient (44% yield), subsequent attempts at Prins cyclization with the terminal alkyne unprotected were unsuccessful. In contrast, treatment of **25** with TMSI gave the 4-iodo tetrahydropyran **26** in 88% yield as a single stereoisomer. Radical deiodination of **26** with $\text{Bu}_3\text{SnH}/\text{AIBN}$ followed by TMS cleavage with $\text{K}_2\text{CO}_3/\text{MeOH}$ then provided alkyne **27** in high overall yield (85% from **26**).



Scheme 4. Synthesis of alcohol **11b**: a) 3-TMS-propionic acid, DCC, DMAP, DCM, -20°C , 38%; b) DIBAL–H, then Ac_2O , pyridine, DMAP, DCM, -78°C , 89%; c) TMSI, 2,6-dimethylpyridine (20 mol%), DCM, -20°C to RT, 88%; d) Bu_3SnH , AIBN (10 mol%), toluene, reflux, 87%; e) K_2CO_3 , MeOH, RT, 98%; f) **28**, $n\text{BuLi}$, $\text{BF}_3\cdot\text{Et}_2\text{O}$, THF, -78°C , 83%; g) LiAlH_4 , THF, 50°C , 56%; h) TBDPSCI, imidazole, DMF, RT, 92%.



Scheme 5. Final steps of the synthesis of (–)-zampanolide analogs 5–8: a) 2,4,6-Trichlorobenzoyl chloride, NEt_3 , DMAP, toluene, RT, 74–88%; b) HF-py, THF, 0 °C to RT, 73–90%; c) DMP, DCM, RT, 86–98%; d) $\text{Ba}(\text{OH})_2 \cdot \text{THF}/\text{H}_2\text{O}$ (40:1), RT, 64–76%; e) DDQ, DCM/ H_2O (5:1), RT, 62–97%; f) DMP, DCM, 67–95%; g) (S)-BINOL, LiAlH_4 , EtOH, (Z,E)-sorbamide, THF, RT, 15–75 min, 24–71%. For the structures of analogs 5–8 (see Figure 2). For the structures of alcohols 11 a/b, of acids 10a–c, and of acid 10d (see Schemes 1–3, respectively). Analog 5 is derived from acid 10a and alcohol 11b, analogs 6–8 are all derived from alcohol 11a and acids 10b, 10c, and 10d, respectively.

In analogy to our previous synthesis of alcohol 11a,^[35] the projected elaboration of alkyne 27 into 11b was to involve its conversion into a terminal vinyl iodide followed by iodine-lithium exchange and reaction of the ensuing vinyl lithium species with epoxide 28^[49] (Scheme 4). Unfortunately, hydrozirconation/iodination of 27 gave the desired vinyl iodide only in poor yield and with low selectivity. Moreover, treatment of the mixture of vinyl iodides in toluene with *n*BuLi followed by addition of epoxide 28 in the presence of $\text{BF}_3 \cdot \text{Et}_2\text{O}$ led to a complex mixture of products.

As an alternative to the use of a vinylmetal in the epoxide opening reaction, we then investigated the reaction of lithiated alkyne 27 and epoxide 28 in the presence of $\text{BF}_3 \cdot \text{Et}_2\text{O}$ in THF.^[50] In the event, the corresponding homopropargylic alcohol was obtained in excellent yield (83%). Hydroalumination of the latter with LAH after aqueous work-up delivered the desired *E* olefin as a single stereoisomer, albeit with concomitant loss of the TBDPS protecting group. However, the resulting diol could be selectively mono TBDPS-protected by reaction with TBDPSCI to give alcohol 11b in 50% overall yield from alkyne 27.

Elaboration of analogs 5–8

As depicted in Scheme 5, the elaboration of acids 10a–d and alcohols 11a–b into analogs 5–8 followed the overall strategy outlined in Scheme 1. Thus, esterification of an acid 10 with an alcohol 11 under Yamaguchi conditions^[51] delivered an ester 29 in yields between 74% and 88%. Global desilylation of 29 with HF-pyridine (73–90%) followed by DMP oxidation^[47] of the resulting diols gave crude phosphono-aldehydes 13 in excellent overall yields (86–98%).

Gratifyingly, when treated with $\text{Ba}(\text{OH})_2 \cdot \text{H}_2\text{O}$ in wet THF^[35] all phosphono-aldehydes 12 underwent efficient intramolecular

HWE reaction, to form macrolactones 30 in yields between 64 and 76%. PMB-cleavage with DDQ and subsequent DMP oxidation of the resulting free alcohols furnished (–)-dactyloide analogs 13.

With (–)-dactyloide analogs 13 in hand, the stage was set for the diastereoselective aza-aldol reaction that would complete the hemiaminal linked side chain at C(19). Following a protocol that we have recently reported for the stereoselective addition of (Z,E)-sorbamide to dactyloide analogs,^[45] aldehydes 13 were reacted with an in situ formed (S)-BINAL-sorbamide complex to deliver zampanolide analogs 5–8 in yields between 24 (8) and 71% (6) and *dr* values of >93:7 (at C(20)) after flash column chromatography and subsequent NP-HPLC purification. (For details, see the Supporting Information.) As an exception, analog 8 was only purified by flash column chromatography, as decomposition was observed during attempted NP- or RP-HPLC purification; likewise, slow retro aza-aldol reaction was detectable for 8 in CDCl_3 solution. Analog 7 was obtained as an inseparable 1.4:1 mixture of diastereoisomers at C(5).

For analog 5, the relative and absolute configuration of all stereocenters could be confirmed by X-ray crystallography (Figure 3),^[53] notably, no other crystal structure of a zampanolide-type molecule has been reported in the literature so far. Most importantly, the structural data firmly establish that the asymmetric aza-aldol reaction between aldehydes 13 and the amide transfer reagent derived from sorbamide and (S)-BINOL produces an (S)-configured C(20) stereocenter. It is also worth noting that the crystal structure of 5 shows an *s-trans* conformation of the enone moiety, which is in line with previous findings by Taylor and co-workers on the conformational preferences of (–)-dactyloide (2) in DMSO solution (with an approximately 70% fraction of *s-trans* conformers present in the conformational equilibrium).^[44,52] Interestingly, however, the reaction of zampanolide with His229 of β -tubulin must occur

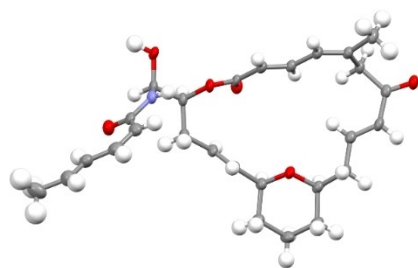
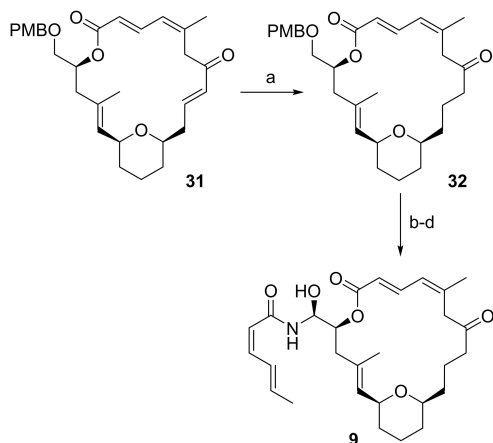


Figure 3. X-ray crystal structure of 13-desmethylene-17-desmethyl-(–)-zampanolide (**5**).

from an *s-cis* conformation, based on the configuration of the newly formed stereocenter in the adduct.^[31]

Analog **9** was obtained from macrolactone **31**, which we had previously prepared as part of our synthesis of 13-desmethylene-(–)-zampanolide (**3**; Scheme 6).^[45] Selective reduction of the enone double bond in **31** with Stryker's reagent^[54] furnished



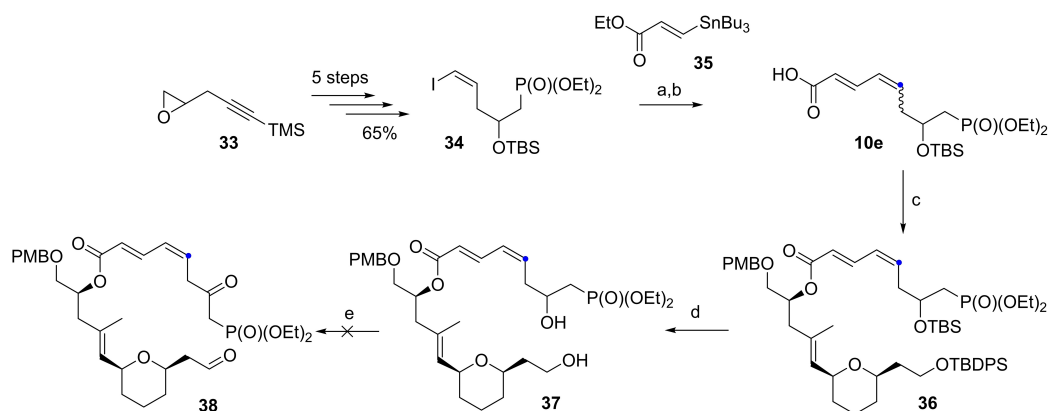
Scheme 6. Synthesis of analog **9**: a) $(\text{PPh}_3\text{CuH})_6$, toluene, -40°C , 65%; b) DDQ, DCM/ H_2O (5:1), RT, 79%; c) DMP, DCM, 74%; d) (*S*)-BINOL, LiAlH_4 , EtOH, (*Z,E*)-sorbamide, THF, RT, 15–75 min, 54%.

macrocyclic ketone **32** in 65% yield. The latter was then elaborated into analog **9** by PMB-deprotection, DMP oxidation and aza-aldol reaction in 32% overall yield. Analog **9** was obtained with a *dr* of 88:12.

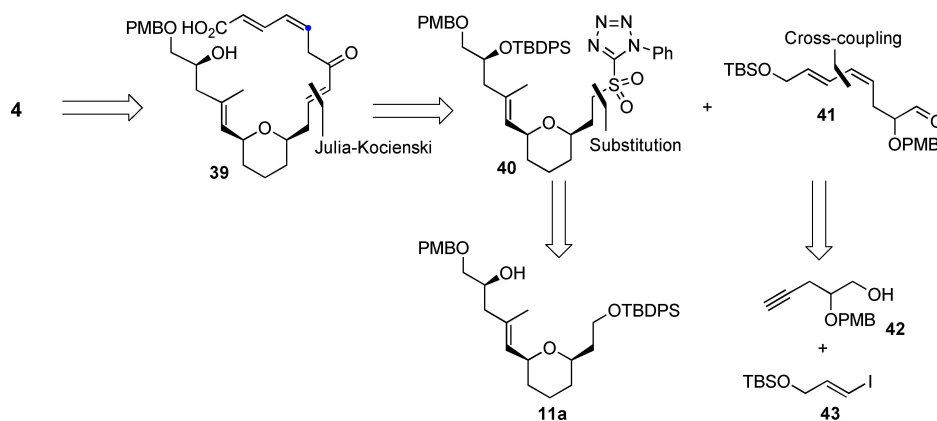
Studies towards the synthesis of analog 4: Synthesis of 5-desmethyl-13-desmethylene-(–)-dactylolide

Attempted macrocyclization by intramolecular HWE olefination

As for the synthesis of analogs **5–9**, our initial plan for the synthesis of analog **4** was based on the general strategy outlined in Scheme 1 and thus envisaged the assembly of the heavy atom framework of the macrocycle by the esterification of alcohol **11a** with acid **10e**. As depicted in Scheme 7, acid **10e** was assembled by Stille coupling of ester **35**^[55] and vinyl iodide **34** as the key step. The latter could be accessed from (racemic) epoxide **33**^[56] in 5 steps, including $\text{BF}_3 \cdot \text{Et}_2\text{O}$ -mediated epoxide opening with lithium diethylphosphite in THF at -78°C , TBS-protection of the ensuing free hydroxy group, TMS-removal with K_2CO_3 in methanol, reaction of the terminal triple bond with NIS in the presence of catalytic AgNO_3 in acetone, to produce an iodoalkyne, and, finally, treatment of the latter with 2-nitrobenzenesulfonylhydrazide and Et_3N (as an in situ source of diimide^[57]); **34** was obtained in excellent overall yield (65%), although it was contaminated with about 20% of the corresponding alkyl iodide, resulting from over-reduction of the precursor iodoalkyne. Stille coupling of this material with **35** produced the corresponding *E/Z*-enoate in 70% yield, with the alkyl iodide contaminant being readily separable at this stage by flash chromatography. Saponification of the coupling product with aqueous sodium hydroxide in ethanol then gave the desired carboxylic acid **10e** in 68% yield, on a 300 mg scale. Surprisingly, when the reaction was repeated on a 1 g scale under ostensibly identical conditions, extensive isomerization of the C(4)=C(5) double bond was observed, leading to an approximately 1:1 mixture of **10e** and its *E/E* isomer. The reasons for this discrepancy are unclear and no efforts were



Scheme 7. a) **35**, Pd_2dba_3 , DIPEA, NMP, RT, dark, 70%; b) NaOH, EtOH, RT, 76% (up to 50% isomerization of the *Z* double bond); c) TCBC, Et_3N , toluene, DMAP, RT, 68%; d) HF-py, py, THF, RT, 98%; e) DMP, DCM, RT, decomposition.



Scheme 8. Macrolactonization-based retrosynthesis of zampanolide analog 4.

made to finetune the reaction conditions such as to prevent isomerization also on a larger scale.

As for the previous analogs described, the esterification of **10e** with alcohol **11a** was performed under Yamaguchi conditions,^[51] which furnished ester **36** in 69% yield. When the esterification was performed with a mixture of **10e** and its *E/E* isomer a mixture of the corresponding esters was obtained in 68% total yield without noticeable change in isomer ratio. Gratifyingly, the desired ester **36** was separable from its *E/E* isomer at this stage by column chromatography. Ester **36** was then submitted to global desilylation with pyridine-buffered HF-pyridine in THF to yield diol **37** in 98% yield. However, while oxidation of this diol with DMP did occur (as indicated by in-process reaction monitoring with TLC-MS and NMR), the desired keto aldehyde could not be isolated after work-up. More specifically, the organic layer turned dark red during work-up and no product-related signals could be detected in the ¹H-NMR spectrum of the crude material recovered from the organic phase. In order to avoid problems that might be related to aqueous work-up conditions, activated Ba(OH)₂ in wet THF was added directly to the reaction mixture after completion of the DMP oxidation. Unfortunately, immediate decomposition was observed and none of the desired macrocycle could be isolated.

Macrolactonization approach

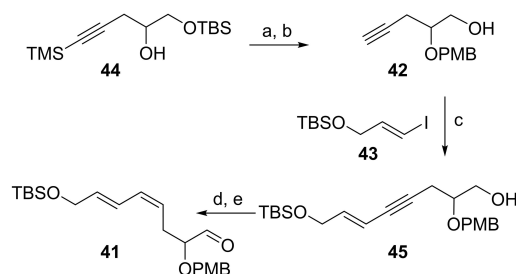
In light of the difficulties encountered with the HWE-based macrocyclization approach towards 13-desmethylene-5-desmethyl-(–)-zampanolide (**4**), we started to explore an alternative overall strategy that would involve macrocyclic ring-closure by macrolactonization rather than double bond formation between C(8) and C(9) (Scheme 8). The requisite *seco* acid **39** was envisioned to be prepared by means of Julia-Kocienski olefination^[58] from aldehyde **41** and sulfone **40**.

Aldehyde **41** was projected to be obtained by Sonogashira cross-coupling^[59] of **42** and **43** followed by semireduction of the triple bond. Sulfone **40** would be obtained from alcohol **11a** following previous work by Smith and co-workers.^[36] In the forward direction, the elaboration of aldehyde **41** made use of

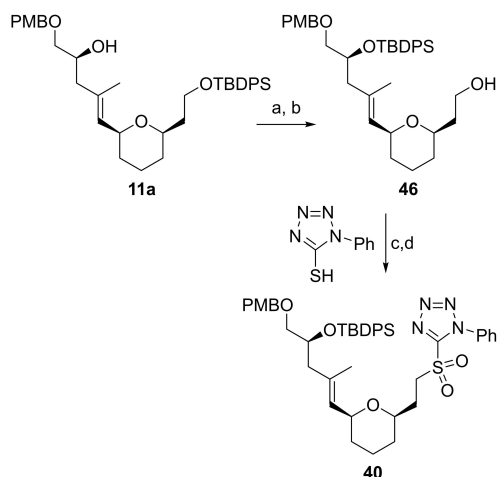
homopropargylic alcohol **44**,^[60] which was transformed into **42** by PMB-protection and subsequent desilylation with TBAF·3H₂O in THF in 74% overall yield (Scheme 9).

Sonogashira coupling^[59] of **42** with vinyl iodide **43**^[61] efficiently delivered enyne **45** (98% yield). The alkyne moiety was then selectively reduced to the *Z* double bond with freshly prepared Zn/Cu/Ag composite that was activated with TMSCl.^[62] To obtain full conversion, the reaction had to be heated to 55 °C for three days, thus furnishing the corresponding diene in 84% yield. Finally, the ensuing diene was oxidized under buffered Dess–Martin conditions to give aldehyde **41**, which proved to be rather unstable. The conversion of alcohol **11a** into sulfone **40** in a first step involved TBDPS-protection of the free secondary hydroxy group, followed by selective cleavage of the primary TBDPS-ether with TBAF/AcOH, to furnish **46** in 52% overall yield (Scheme 10). Treatment of **46** with 1-phenyl-1*H*-tetrazol-5-thiol under Mitsunobu conditions^[63] then furnished a thioether that was oxidized to the corresponding sulfone **40** with hydrogen peroxide in the presence of catalytic amounts of (NH₄)₆Mo₇O₂₄·4H₂O in ethanol.^[36] Sulfone **40** was obtained in 80% overall yield from alcohol **46**.

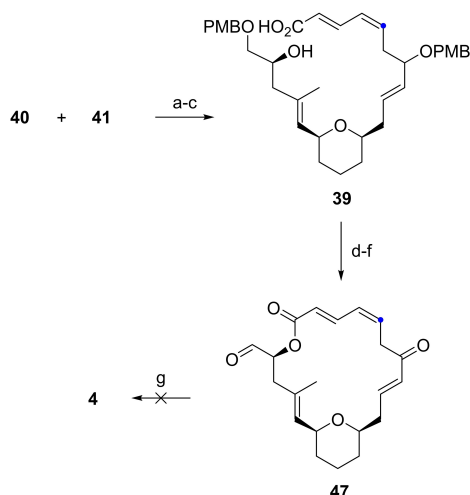
The Julia–Kocienski olefination of **40** and aldehyde **41** proceeded smoothly and delivered the desired olefin in 82% yield as a single isomer (Scheme 11). Double desilylation with HF-pyridine then gave the corresponding free diol in 64% yield;



Scheme 9. Synthesis of aldehyde **41**: a) PMB-trichloroacetimidate, TFOH (2.0 mol%), Et₂O, RT, 93%; b) TBAF·3H₂O, THF, RT, 80%; c) **43**, Pd(PPh₃)₄, CuI, Et₃N, MeCN, 45 °C, 98%; d) Zn/Cu/Ag, TMSCl, MeOH, THF, H₂O, 55 °C, 3 d, 84%; e) DMP, NaHCO₃, DCM, RT, 69%.



Scheme 10. a) Synthesis of sulfone **40**: TBDPSCI, imidazole, DCM, RT, 91%; b) TBAF/AcOH, THF, 57%; c) 1-phenyl-1*H*-tetrazol-5-thiol, PPh₃, DEAD, THF, 0 °C, 92%; d) H₂O₂ (aq.), (NH₄)₆Mo₇O₂₄·4H₂O (10 mol %), EtOH, RT, 88%.



Scheme 11. Final steps in the synthesis of 13-desmethylene-5-desmethyl-(-)-dactylolide (**47**): a) **40**, KHMDS, THF, -78 °C, then aldehyde **41**, 82%; b) HF-py, THF, RT, 64%; c) MnO₂, DCM, RT, then NaClO₂, resorcinol, *t*BuOH, acetate buffer pH 4.0, 5 d, 74%; d) TCBC, Et₃N, THF, RT, DMAP, Et₃N, toluene, 69%; e) DDQ, DCM/buffer pH 7.2, RT, 65%; f) DMP, NaHCO₃, DCM, RT, 87%; g) (S)-BINOL, LiAlH₄, EtOH, (Z,E)-sorbamide, THF, RT, decomposition.

selective oxidation of the allylic hydroxy group with MnO₂ followed by immediate Pinnick oxidation of the ensuing aldehyde subsequently furnished acid **39**. To avoid isomerization of the *E,Z*-dienal, a modified variant of the Pinnick oxidation was employed that used resorcinol as a scavenger.^[63] While the reaction was slow and took up to five days to reach > 90% conversion, no isomerization of the *Z* double bond occurred under the modified Pinnick conditions and *seco* acid **39** was isolated in 74% overall yield (based on the preceding diol). Gratifyingly, treatment of *seco* acid **39** with 2,4,6-trichlorobenzoic acid, Et₃N and DMAP^[51] led to smooth macro-lactonization (69% yield); simultaneous cleavage of the two PMB-ether groups with DDQ followed by DMP oxidation of the resulting diol then furnished 5-desmethyl-13-desmethyl-(-)-dactylolide (**47**) in 39% overall yield from **39**. Unfortunately, all attempts to convert **47** into 13-desmethylene-5-desmethyl-(-)-zampanolide (**4**) by applying our stereoselective aza-aldol reaction protocol^[45] proved to be futile. Only decomposition of the starting material **47** was observed.

Cellular effects of zampanolide analogs 5–9

As touched upon in the Introduction, we have shown previously that 13-desmethylene-(-)-zampanolide (**3**) was an equally potent growth inhibitor of A549, A2780 and A2780AD cells as natural (-)-zampanolide (**1**).^[45] In this study we have now extended the profiling of **3** to 5 additional cancer cell lines (HL-60, 1A9, MCF-7, PC-3, and HT29; Table 1) and the data obtained have reconfirmed that **3** is a highly potent inhibitor of cancer cell proliferation *in vitro*; in all cases investigated so far, the activity of **3** was at least comparable with that of natural (-)-zampanolide (**1**). These results are in agreement with and extend previous findings on 13-desmethylene-(-)-dactylolide (**3**)^[35] and they clearly indicate that the C(13)-exomethylene group is not essential for the biological activity of zampanolide-type structures.

Of the different analogs of **3**, the two dihydro derivatives **6** and **9** showed dramatically different activities (Table 1). While 8,9-dihydro analog **9** was consistently several hundred times less potent than **3**, the 2,3-dihydro derivative **6** retained at least double-digit nanomolar potency against all six cell lines investigated here. For four of these cell lines (A2780, A2780AD, HL-60, 1A9), the IC₅₀ values for analog **6** were no more than

Table 1. Antiproliferative activity of (-)-zampanolide (**1**) and zampanolide analogs **3**, and **5–9** against human cancer cell lines (IC₅₀ [nM]).^[a]

Cpd	A549 (lung)	A2780 (ovarian)	A2780AD ^[b] (ovarian) ¹	HL-60 (leukemia)	1A9 (ovarian)	HT29 (colon)	MCF-7 ^[c] (breast)	PC3 ^[c] (prostate)
1	3.2 ± 0.4 ³⁵	1.9 ± 0.2 ³⁰	2.2 ± 0.3 ³⁰	4.1 ± 0.5	15 ± 8	1.87 ± 0.38	n.d.	n.d.
3	1.0 ± 0.2	1.7 ± 0.4	3.53 ± 1.97	2.5 ± 0.6	12 ± 5	1.24 ± 0.20	< 1.5	< 1.5
5	15 ± 5	13 ± 1	20 ± 4	26 ± 6	90 ± 23	32.9 ± 2.56	n.d.	n.d.
6	44 ± 10	5.2 ± 0.6	12 ± 3	5.9 ± 1	16 ± 5	10.85 ± 0.49	n.d.	n.d.
7	133 ± 6	65 ± 21	72 ± 28	n.d.	n.d.	n.d.	n.d.	n.d.
8	120 ± 8	110 ± 21	94 ± 4	n.d.	n.d.	n.d.	n.d.	n.d.
9	1056 ± 50	820 ± 20	1860 ± 890	2910 ± 34	9386 ± 2435	684 ± 77	n.d.	n.d.

[a] Cells were exposed to compounds for 48 h (A549, A2780, A2780AD, HL60) or 72 h (1A9, HT29, MCF-7, PC3); n.d. = not determined. [b] Multidrug-resistant cell line overexpressing the Pgp efflux pump.^[66,67] [c] These experiments were conducted at ProQuinase GmbH, Freiburg, Germany.

three times higher than for the parent compound **3**; a slightly more pronounced decrease in potency (sixfold) was observed against HT29 cells, while A549 cells were 44 times less sensitive to **6** than **3**.

The potency loss incurred by **9** is not too surprising, as the compound lacks the reactive enone system that is responsible for the covalent interaction of (–)-zampanolide (**1**) with tubulin; but the data provide additional experimental confirmation that the covalent nature of the interaction of **1** (and **3**, for that matter) with the protein is truly essential for high cellular potency. This conclusion has also been reached independently by Taufa et al. based on the activity of the recently isolated zampanolide E (8,9-dihydro-(–)-zampanolide) against HL-60 cells.^[27] Based on the cell cycle and microtubule bundling data discussed below, the residual activity of **9** and zampanolide E is most likely due to noncovalent binding to tubulin; but we cannot completely exclude the involvement of other cellular targets.

The high potency of **6** is intriguing, as the formal reduction of the double bond would be expected to increase the flexibility of the structure and, thus, enhance the entropic cost of target binding. However, we have previously found for other bioactive macrocycles (3-deoxy-2,3-didehydro-epothilone A,^[65] rhizoxin F (M. Liniger, C. Neuhaus, K.-H. Altmann, unpublished data) that the formal reduction of *E* double bonds was associated only with a moderate loss in cellular potency.

Removing both the C(2)=C(3) and the C(4)=C(5) double bond simultaneously, led to a further three- to 12-fold decrease in potency for analog **7** (compared to **6**); interestingly, no further drop in activity was observed upon removal of the C(5) methyl group from **7** (i.e., for analog **8**). While analogs **7** and **8** thus appear to be one to two orders of magnitude less potent than **3**, both compounds still exhibit profound antiproliferative activity. Given the removal of the two C=C double bonds from the dienone system in the northern part of the structure of **3**, this finding is quite remarkable. It should also be noted that analog **7** represents a 1.4:1 mixture of diastereoisomers at C(5); if one of these isomers were substantially more potent than the other, the IC₅₀ values of the former could be up to 2.4 times lower than those for the mixture.

The removal of the C(17) methyl group (analog **5**) was associated with a six- to 26-fold potency loss versus **3** (Table 1). The compound, thus, is somewhat less potent than **6**, but it still exhibits high antiproliferative activity. For reasons that cannot be discerned, the IC₅₀ values obtained here for **5** against A549 and 1A9 cells are lower than those reported by Taylor and co-workers, even if one takes into account that Taylor's study was performed with a 1.5:1 epimeric mixture at C(20).

Finally, for all analogs, similar activity was observed against the ovarian cancer cell line A2780 and its Pgp-overexpressing, multidrug-resistant A2780AD variant.^[65,66] Similar findings have been made previously for natural (–)-zampanolide (**1**)^[30] and for **3**.^[45] The ability of zampanolide-type structures to overcome Pgp-mediated multidrug-resistance may be a direct consequence of their covalent mode of action, which leads to irreversible intracellular retention. Whether, in addition, they

might also be intrinsically poor substrates for the Pgp efflux pump has not been determined.

As discussed above, C(5)-desmethyl-C(13)-desmethylene-(–)-zampanolide (**4**) was not accessible through either of the two strategies investigated. However, experiments with C(5)-desmethyl-C(13)-desmethylene-(–)-dactylolide (**47**) on 1A9 and HT29 cells revealed an approximately ten- or 30-fold loss in potency, respectively, relative to (–)-dactylolide (**2**) (IC₅₀ values 1A9 cells: **47**, 8.34 ± 0.95 μM; **2**, 0.82 ± 0.14 μM. IC₅₀s HT29 cells: **47**, 10.56 ± 0.28 μM; **2**, 0.359 ± 0.083 μM). These potency differences are comparable with those observed between **5** and **3**, which may suggest that the activities of **5** and the elusive **4** may be similar. However, this conclusion has to be considered tentative, as it is not clear if the same macrocycle modification in (–)-dactylolide (**2**) and (–)-zampanolide (**1**) leads to the same relative change in potency.

The antiproliferative activity of zampanolide analogs is reflective of their effects on the cellular microtubule network and on cell cycle progression. As shown in Figure 4, 13-desmethylene-(–)-zampanolide (**3**) at a concentration of 25 nM induced microtubule bundling in interphase cells similar to what was observed with 200 nM taxol and what had been reported for (–)-zampanolide (**1**). Likewise, microtubule bundling was also observed with analogs **5** and **6** at similar concentrations (Figure S10).

In comparison, and as expected from its significantly lower growth inhibitory activity, 13-desmethylene-8,9-dihydro-(–)-zampanolide (**9**) led to microtubule bundling only at substantially higher concentrations (5 μM; Figure 4). Nevertheless, this finding indicates that the antiproliferative effects of **9** are still mediated through interaction with the tubulin/microtubule system (at least partly). Notably, the effects of short term exposure (6 h) of A549 cells to 5 μM of **9** were fully reversible, as was also the case for taxol; in contrast, no reversibility was observed with **3**, **5**, or **6**, all of which incorporate the reactive enone system that enables covalent attachment to β-tubulin.

In line with their effects on the microtubule cytoskeleton, the treatment of A549 cells with analogs **3**, **5**, or **6** led to cell cycle arrest in the G2/M phase at low-nanomolar concentrations (Figure 5), as has also been demonstrated for (–)-zampanolide (**1**).^[28] Mitotic arrest was also observed with analog **9**, but only at much higher compound concentrations (25 μM; Figure 5).

Binding to microtubules and promotion of tubulin polymerization

In order to gain some basic understanding of the effects of the various modifications of **3** on the interaction of the corresponding zampanolide analogs with tubulin, we have investigated their ability to displace the fluorescent taxol analog Flutax-2 from preformed crosslinked microtubules.^[68]

For noncovalent microtubule binders, the concentration-dependent displacement of Flutax-2 (at a fixed concentration) allows to determine thermodynamic binding constants (*K_b*); conducting these experiments with a covalent microtubule ligand (which is formally treated like a reversible ligand) only

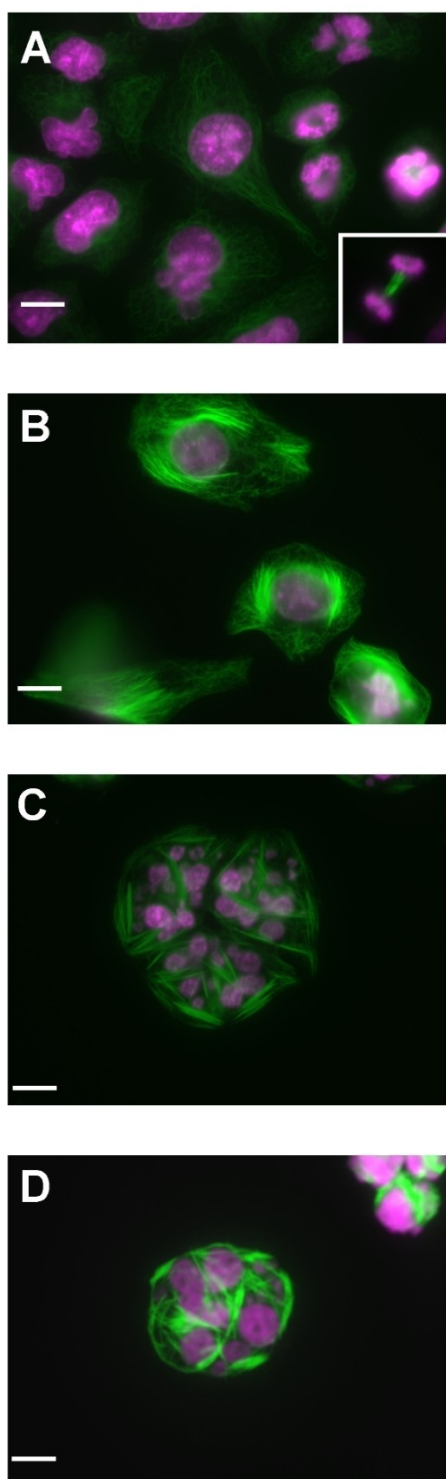


Figure 4. Microtubule bundling in A549 cells induced by 13-desmethylene-(–)-zampanolide (**3**) and its 8,9-dihydro derivative (**9**). Microtubule (green) and DNA (pink) staining of A549 lung carcinoma cells. Cells were treated with A) DMSO (negative control), B) taxol (200 nM, positive control), C) **3** (25 nM), or D) 5 μ M of **9**. Microtubules were immunostained with an α -tubulin monoclonal antibody; DNA was stained with Hoechst 33342. Scale bars: 10 μ m.

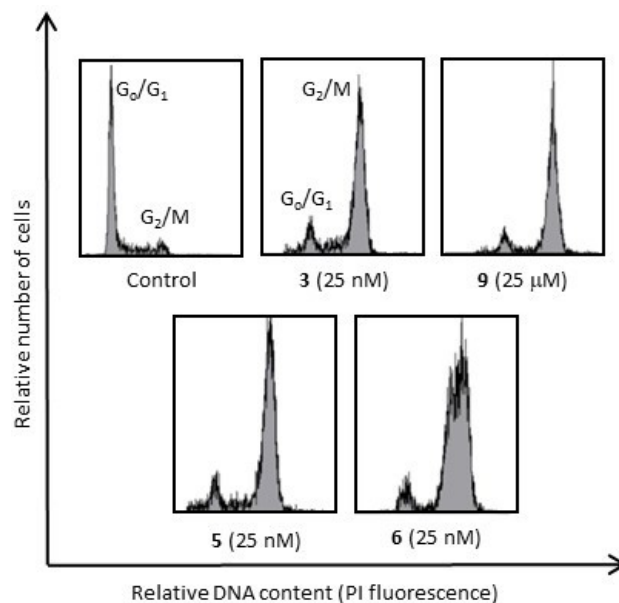


Figure 5. Cell-cycle histograms of A549 lung carcinoma cells treated with compounds **3**, **5**, **6**, or **9**. Shown are the lowest ligand concentrations that induce maximal arrest in the G2/M phase.

gives what we refer to as apparent binding constants ($K_{b,app}$). These apparent binding constants do not reflect an equilibrium binding situation, as they depend on both the intrinsic binding affinity of the ligand for tubulin *and* the rate of the subsequent reaction of the ligand with the protein. Thus, $K_{b,app}$ values are less informative than true binding constants K_b and they cannot be directly compared to each other or to true K_b values. However, if one assumes that the tubulin-bound conformation of all zampanolide analogs investigated here is similar and that this leads to a similar rate constant for the conversion of the initial noncovalent complex into the covalent adduct, then the differences in $K_{b,app}$ between different zampanolide analogs provide at least an approximate measure for the differences in intrinsic binding affinity. Independent of these assumptions, $K_{b,app}$ values provide a measure for the efficiency of the overall reaction of zampanolide analogs with polymerized tubulin.

The $K_{b,app}$ values for zampanolide analogs **3**, **5**, **6**, **7**, and **8** are summarized in Table 2; for analog **9** the value is a true thermodynamic binding constant. It is immediately obvious that analogs **5**–**8** are all less efficient than 13-desmethylene-(–)-zampanolide (**3**) in displacing Flutax-2 from stabilized micro-

Table 2. Apparent microtubule binding constants $K_{b,app}$ of (–)-zampanolide (**1**) and analogs **3** and **5**–**9** for microtubules at 35 °C.

Cpd	$K_{b,app}$ [10^6 M^{-1}] ^[a]	Cmpd	$K_{b,app}$ [10^6 M^{-1}] ^[a]
1 ^[b]	214 ± 9.3	3	24 ± 2
5	1.9 ± 0.4	6	7 ± 2
7	0.47 ± 0.07	8	2.29 ± 0.2
9	0.061 ± 0.001		

[a] Determined by the displacement of the fluorescent taxoid Flutax-2 from stabilized microtubules.^[68] [b] Data are from ref. [30].

tubules. In comparison to **3**, the smallest difference in $K_{b,app}$ values (ca. 3.6-fold) was observed for 13-desmethylene-2,3-dihydro-(–)-zampanolide (**6**), for all other analogs $K_{b,app}$ was reduced more than tenfold. The data indicate that all modifications to **3** compromise the microtubule-binding affinity of the corresponding analogs to some extent.

Conclusions

C(13)-Desmethylene-(–)-zampanolide (**3**) is an equipotent, synthetic congener of the marine microtubule stabilizer (–)-zampanolide (**1**). In this study, we have investigated the importance of individual double bonds and of the C(17) methyl group in **3** (and, by inference, in (–)-zampanolide (**1**)) for its antiproliferative activity and interactions with microtubules. To this end, we have prepared five analogs of **3/1**, including the known C(13)-desmethylene-C(17)-desmethyl-(–)-zampanolide (**5**),^[44] based on a global strategy that we had previously elaborated for the total synthesis of **1** and **3**. The successful and efficient preparation of these analogs attests to the robustness of our synthetic approach; in particular, in all cases the intramolecular HWE reaction of phosphono aldehydes **12**, which has also been adopted by others,^[40–44] provided the desired macrocycles in good yields. In addition, the C(20) stereocenter could be established with high selectivity, employing a putative (S)-BINOL-based amide transfer reagent that we have recently developed. As the only exception, 5-desmethyl-(–)-dactylolide (**47**) could not be converted into the corresponding zampanolide analog **4**, which has remained elusive in this study. Likewise, a macrolactonization-based approach had to be developed to access **47**, as the ω -oxo β -keto phosphonate **38**, as the requisite precursor for an HWE-based macrocyclization could not be obtained in this case by oxidation of the corresponding diol **37**.

C(13)-Desmethylene-(–)-zampanolide (**3**) proved to be an equally potent inhibitor of cancer cell growth as (–)-zampanolide (**1**) across a panel of six tumor cell lines. All structural modifications of **3** investigated here led to a decrease in cellular potency, albeit to a different extent. Overall, the best-tolerated modification was the formal reduction of the C(2)=C(3) double bond; with the exception of one cell line, the corresponding analog **6** was no more than six times less active than **3**. A more pronounced, but still moderate, loss in potency was caused by the removal of the C(17)-methyl group.

All synthetic zampanolides, including 13-desmethylene-(–)-zampanolide (**3**) were less efficient in displacing the fluorescent taxoid Flutax-2 from the taxol binding site on stabilized microtubules, as judged by their apparent binding constants $K_{b,app}$. The interpretation of the displacement data is not straightforward, as the derived $K_{b,app}$ values are not equilibrium binding constants. However, they seem to suggest that all modifications, including the removal of the C(13) methylene group, reduce the stability of the initial, noncovalent ligand-tubulin complex relative to natural (–)-zampanolide (**1**). This conclusion is in line with the fact that both the C(13)-methylene or the C(17)-methyl group are located in hydrophobic pockets

in the protein.^{[31][69]} In addition, as has been elegantly demonstrated by Taylor and co-workers by computational and solution NMR studies on C(17)-desmethyl-(–)-dactylolide, removal of the C(17)-methyl group leads to greater conformational flexibility in the C(14)–C(19) segment of the macrocycle,^[44] which might additionally compromise microtubule-binding affinity. Enhanced conformational flexibility could also explain the reduced binding affinity of analogs **6–8**, although for **6** the decrease in $K_{b,app}$ versus **3** is rather moderate. This assumption is supported by the results of macrocycle conformation sampling using the Schrödinger OPLS4 force field and subsequent clustering of 3000 to 5000 conformations for each analog based on macrocycle atoms. (For details see the Supporting Information.) According to these computations, all analogs of **3** generally exhibit greater conformational flexibility than **1** in the regions surrounding the modifications, but not in other parts of the structure. For analog **5**, these observations are nicely aligned with the results of Taylor's work.^[44] Conformational flexibility was found to be most pronounced for analog **9**, while the sampled conformational space is virtually identical for **1** and **3**.

In spite of its tenfold lower $K_{b,app}$ compared to **1**, C(13)-desmethylene-(–)-zampanolide (**3**) is equipotent with **1** on cells; likewise, analogs **5** and **6** exhibit high cellular potency. We believe that the correlation between apparent binding constants and cellular activity is blurred by the irreversible binding of analogs **5–8** to microtubules, as compounds with only moderately reduced $K_{b,app}$ can achieve levels of tubulin labelling approaching those of **1** within the timeframe of the cellular experiments. More detailed studies will be necessary to consolidate (or refute) this hypothesis (see, however, ref. [70]).

Finally, it needs to be noted that Johnson, Risinger and co-workers have recently reported the first in vivo data with (–)-zampanolide (**1**) in tumor-bearing mice.^[70] In this study, **1** was found to exhibit profound antitumor activity when administered intratumorally; however, even a single i.p. dose of 1 mg/kg proved to be highly toxic without showing any antitumor activity. The absence of a systemic therapeutic window for **1** is disappointing. However, the unique mechanism of action of zampanolide-type structures and their activity against MDR tumor cells still makes the continued evaluation of analogs of **1** a worthwhile undertaking. In this context, the in vivo evaluation of some of the analogs described in this study would help to understand whether structurally modified and somewhat less potent analogs of **1** could offer an acceptable therapeutic window.

Experimental Section

For all experimental details see the Supporting Information. Additional references are cited within the Supporting Information.^[71–85]

Acknowledgements

This work was supported by the Swiss National Science Foundation (KHA, project 200021_149253). Institutional support

by the ETH Zurich is also gratefully acknowledged (KHA). Funding was also received from Ministerio de Ciencia e Innovación (Spain) (JFD, Project PID2019-104545RB100/AEI/10.13039/501100011033), the European Commission-NextGenerationsEU (Regulation EU 2020/2094), through CSIC's Global Health Platform (PTI Salud Global) and Proyecto de Investigación en Neurociencia Fundación Tatiana Pérez de Guzmán el Bueno 2020 (JFD). Salary funding was received from Victoria University's Strategic Investment fund (CD), and general funding was received from the Cancer Society of NZ and the Wellington Medical Research Foundation (JHM). We are indebted to Dr. Leo Betschart and Dr. Philipp Waser (ETHZ) for NMR support, to Kurt Hauenstein (ETHZ) for technical advice and to Oswald Greter, Louis Bertschi, Michael Meier, and Daniel Wirz (ETHZ) for HRMS spectra acquisition. We are grateful to Dr. Nils Trapp (ETHZ) for solving the X-ray crystal structure of compound 5. We thank Dr Paul Teesdale-Spittle of Victoria University for assistance with the biological assays. Open Access funding provided by Eidgenössische Technische Hochschule Zürich.

Conflict of Interests

The authors declare no conflict of interest.

Data Availability Statement

The data that support the findings of this study are available in the supplementary material of this article.

Keywords: medicinal chemistry · natural products · structure-activity relationships · total synthesis · zampanolide

- [1] D. J. Newman, G. M. Cragg, *J. Nat. Prod.* **2020**, *83*, 770–803.
- [2] S. S. Bharate, S. Mignani, R. A. Vishwakarma, *J. Med. Chem.* **2018**, *61*, 10345–10374.
- [3] E. Patridge, P. Gareiss, M. S. Kinch, D. Hoyer, *Drug Discovery Today* **2016**, *21*, 204–207.
- [4] M. Butler, A. A. B. Robertson, M. A. Cooper, *Nat. Prod. Rep.* **2014**, *31*, 1612–1661.
- [5] U. Lindequist, *Biomol. Ther.* **2016**, *24*, 561–571.
- [6] W. H. Gerwick, B. S. Moore, *Chem. Biol.* **2012**, *19*, 85–98.
- [7] C. R. Pye, M. J. Bertin, R. S. Lokey, W. H. Gerwick, R. G. Linington, *Proc. Natl. Acad. Sci. USA* **2017**, *114*, 5601–5606.
- [8] Y. Hu, J. Chen, G. Hu, J. Yu, X. Zhu, Y. Lin, S. Chen, J. Yuan, *Mar. Drugs* **2015**, *13*, 202–221.
- [9] R. Montaser, H. Luesch, *Future Med. Chem.* **2011**, *3*, 1475–1489.
- [10] N. Papon, B. R. Copp, V. Courdavault, *Biotechnol. Adv.* **2022**, *54*, 107871.
- [11] W. Y. Lu, H. J. Li, Q. Y. Li, Y. C. Wu, *Bioorg. Med. Chem.* **2021**, *35*, 116058.
- [12] C. Jiménez, *ACS Med. Chem. Lett.* **2018**, *9*, 959–961.
- [13] K.-H. Altmann, *Chimia* **2017**, *71*, 646–651.
- [14] <http://www.marinepharmacology.org/>. Accessed Feb. 28, 2023.
- [15] N. Fusetani in *Marine Toxins as Research Tools, Vol. 1*, (Eds.: N. Fusetani, W. R. Kem), Springer, Berlin Heidelberg, **2009**, pp. 1–44.
- [16] T. F. Molinski, D. S. Dalisay, S. L. Lievens, J. P. Saludes, *Nat. Rev. Drug Discovery* **2009**, *8*, 69–85.
- [17] P. E. S. Munekata, M. Pateiro, C. A. Conte-Junior, R. Domínguez, A. Nawaz, N. Walayat, E. M. Fierro, J. M. Lorenzo, *Mar. Drugs* **2021**, *19*, 1–24.
- [18] M. Yu, W. Zheng, B. M. Seletsky, B. A. Littlefield, Y. Kishi, *Ann. Rep. Med. Chem.* **2011**, *46*, 227–241.
- [19] C. Cuevas, A. Francesch, *Nat. Prod. Rep.* **2009**, *26*, 322–337.
- [20] I. Paterson, E. A. Anderson, *Science* **2005**, *310*, 451–453.
- [21] J. I. Tanaka, T. Higa, *Tetrahedron Lett.* **1996**, *37*, 5535–5538.
- [22] T. Matsumoto, M. Yanagiya, S. Maeno, S. Yasuda, *Tetrahedron Lett.* **1968**, *9*, 6297–6300 (Pederin).
- [23] F. Benz, F. Knuesel, J. Nuesch, H. Treichler, W. Voser, R. Nyfeler, W. Keller-Schierlein, *Helv. Chim. Acta* **1974**, *57*, 2459–2477 (Echinocandin B).
- [24] H. Umezawa, S. Kondo, H. Inuma, S. Kunimoto, Y. Ikeda, H. Iwasawa, D. Ikeda, T. Takeuchi, *J. Antibiot.* **1981**, *34*, 1622–1624 (Spargualin).
- [25] N. B. Perry, J. W. Blunt, M. H. G. Munro, L. K. Pannell, *J. Am. Chem. Soc.* **1988**, *110*, 4850–4851 (Mycalamides).
- [26] Review Pederin/Mycalamide family: R. A. Mosey, P. E. Floreancig, *Nat. Prod. Rep.* **2012**, *29*, 980–995.
- [27] T. Taufa, A. J. Singh, C. R. Harland, V. Patel, B. Jones, T. Halafih, J. H. Miller, R. A. Keyzers, P. T. Northcote, *J. Nat. Prod.* **2018**, *81*, 2539–2544.
- [28] J. J. Field, A. J. Singh, A. Kanakkanthara, T. Halafih, P. T. Northcote, J. H. Miller, *J. Med. Chem.* **2009**, *52*, 7328–7332.
- [29] Y. N. Cao, L. L. Zheng, D. Wang, X. X. Liang, F. Gao, X. L. Zhou, *Eur. J. Med. Chem.* **2018**, *143*, 806–828.
- [30] J. J. Field, B. Pera, E. Calvo, A. Canales, D. Zurwerra, C. Trigili, J. Rodríguez-Salarichs, R. Matesanz, A. Kanakkanthara, S. J. Wakefield, A. J. Singh, J. Jiménez-Barbero, P. Northcote, J. H. Miller, J. A. López, E. Hamel, I. Barasoain, K.-H. Altmann, J. F. Díaz, *Chem. Biol.* **2012**, *19*, 686–698.
- [31] A. E. Prota, K. Bargsten, D. Zurwerra, J. J. Field, J. F. Díaz, K.-H. Altmann, M. O. Steinmetz, *Science* **2013**, *339*, 587–590.
- [32] T. R. Hoye, M. Hu, *J. Am. Chem. Soc.* **2003**, *125*, 9576–9577.
- [33] J. Uenishi, T. Iwamoto, J. Tanaka, *Org. Lett.* **2009**, *11*, 3262–3265.
- [34] A. K. Ghosh, X. Cheng, R. Bai, E. Hamel, *Eur. J. Org. Chem.* **2012**, 4130–4139.
- [35] D. Zurwerra, F. Glaus, L. Betschart, J. Schuster, J. Gertsch, W. Ganci, K.-H. Altmann, *Chem. Eur. J.* **2012**, *18*, 16868–16883.
- [36] A. B. Smith, I. G. Safonov, R. M. Corbett, *J. Am. Chem. Soc.* **2002**, *124*, 11102–11113.
- [37] F. Ding, M. P. Jennings, *J. Org. Chem.* **2008**, *73* (15), 5965–5976.
- [38] K. P. Bold, M. Gut, J. Schürmann, D. Lucena-Agell, J. Gertsch, J. F. Díaz, K.-H. Altmann, *Chem. Eur. J.* **2021**, *27*, 5936–5943.
- [39] C. P. Bold, C. Klaus, B. Pfeiffer, J. Schürmann, R. Lombardi, D. Lucena-Agell, J. F. Díaz, K. H. Altmann, *Org. Lett.* **2021**, *23*, 2238–2242.
- [40] G. Chen, R. Wang, B. Vue, M. Patanapongpibul, Q. Zhang, S. Zheng, G. Wang, J. D. White, Q. H. Chen, *Bioorg. Med. Chem.* **2018**, *26*, 3514–3520.
- [41] G. Chen, M. Patanapongpibul, Z. Jiang, Q. Zhang, S. Zheng, G. Wang, J. D. White, Q. H. Chen, *Org. Biomol. Chem.* **2019**, *17*, 3830–3844.
- [42] G. Chen, Z. Jiang, Q. Zhang, G. Wang, Q. H. Chen, *Molecules* **2020**, *25*, 362.
- [43] G. Chen, M. Gonzalez, Z. Jiang, Q. Zhang, G. Wang, Q. H. Chen, *Bioorg. Med. Chem. Lett.* **2021**, *40*, 127970.
- [44] J. L. Henry, M. R. Wilson, M. P. Mulligan, T. R. Quinn, D. L. Sackett, R. E. Taylor, *MedChemComm* **2019**, *10*, 800–805.
- [45] T. M. Brüttsch, S. Berardozi, M. L. Rothe, M. Redondo Horcajo, J. F. Díaz, K.-H. Altmann, *Org. Lett.* **2020**, *22*, 8345–8348.
- [46] A. P. Krapcho, J. F. Weimaster, J. M. Eldridge, E. G. E. Jahngen, A. J. Lovey, W. P. Stephens, *J. Org. Chem.* **1978**, *43*, 138–147.
- [47] D. B. Dess, J. C. Martin, *J. Org. Chem.* **1983**, *48*, 4155–4156.
- [48] J. M. Stevens, D. W. C. MacMillan, *J. Am. Chem. Soc.* **2013**, *135*, 11756–11759.
- [49] K. C. Nicolaou, K. C. Fylaktakidou, H. Monenschein, Y. Li, B. Weyershausen, H. J. Mitchell, H. X. Wei, P. Guntupalli, D. Hepworth, K. Sugita, *J. Am. Chem. Soc.* **2003**, *125*, 15433–15442.
- [50] N. D. Kjeldsen, E. D. Funder, K. V. Gothelf, *Org. Biomol. Chem.* **2014**, *12*, 3679–3685.
- [51] J. Inanaga, K. Hirata, H. Saeki, T. Katsuki, M. Yamaguchi, *Bull. Chem. Soc. Jpn.* **1979**, *52*, 1989–1993.
- [52] E. M. Larsen, M. R. Wilson, J. Zajicek, R. E. Taylor, *Org. Lett.* **2013**, *15*, 5246–5249.
- [53] Deposition Number 1499285 (for 5) contains the supplementary crystallographic data for this paper. These data are provided free of charge by the joint Cambridge Crystallographic Data Centre and Fachinformationszentrum Karlsruhe Access Structures service.
- [54] W. S. Mahoney, D. M. Brestensky, J. M. Stryker, *J. Am. Chem. Soc.* **1988**, *110*, 291–293.
- [55] A. F. Renaldo, J. W. Labadie, J. K. Stille, *Org. Synth.* **1989**, *67*, 86–94.
- [56] D. M. Troast, J. Yuan, J. A. Porco, *Adv. Synth. Catal.* **2008**, *350*, 1701–1711.
- [57] M. Jimenez, W. Zhu, A. Vogt, B. W. Day, D. P. Curran, *Beilstein J. Org. Chem.* **2011**, *7*, 1372–1378.

- [58] For a recent review, see: P. X. T. Rinu, S. Radhika, G. Anilkuma, *ChemistrySelect* **2022**, *7*, e202200760.
- [59] For a review on the use of the Sonogashira coupling in natural product synthesis, see: D. Wang, S. Gao, *Org. Chem. Front.* **2014**, *1*, 556–566.
- [60] J. Franke, M. Bock, R. Dehn, J. Fohrer, S. B. Mhaske, A. Migliorini, A. A. Kanakis, R. Jansen, J. Herrmann, R. Müller, A. Kirschning, *Chem. Eur. J.* **2015**, *21*, 4272–4284.
- [61] C. Spino, M. C. Tremblay, C. Godbout, *Org. Lett.* **2004**, *6*, 2801–2804.
- [62] Y. M. A. Mohamed, T. V. Hansen, *Tetrahedron* **2013**, *69*, 3872–3877.
- [63] K. C. K. Swamy, N. N. B. Kumar, E. Balaraman, K. V. P. P. Kumar, *Chem. Rev.* **2009**, *109*, 2551–2651.
- [64] K. Suzuki, K. Tomooka, E. Katayama, T. Matsumoto, G. ichi Tsuchihashi, *J. Am. Chem. Soc.* **1986**, *108*, 5221–5229.
- [65] M. Erdélyi, B. Pfeiffer, K. Hauenstein, J. Fohrer, J. Gertsch, K.-H. Altmann, T. Carlomagno, *J. Med. Chem.* **2008**, *51*, 1459–1463.
- [66] A. M. Rogan, T. C. Hamilton, R. C. Young, R. W. Klecker, R. F. Ozols, *Science* **1984**, *224*, 994–996.
- [67] R. J. Kowalski, P. Giannakakou, S. P. Gunasekera, R. E. Longley, B. W. Day, E. Hamel, *Mol. Pharmacol.* **1997**, *52*, 613–622.
- [68] R. M. Buey, J. F. Díaz, J. M. Andreu, A. O'Brate, P. Giannakakou, K. C. Nicolaou, P. K. Sasmal, A. Ritzén, K. Namoto, *Chem. Biol.* **2004**, *11*, 235–236.
- [69] In spite of its location in a hydrophobic pocket, we had previously assumed that the C(13) methylene group of **1** was not involved in major interactions with the protein.^[39] In light of the binding data for **3** this view may need to be revised.
- [70] L. Takahashi-Ruiz, J. D. Morris, P. Crews, T. A. Johnson, A. L. Risinger, *Molecules* **2022**, *27*, 4244.
- [71] D. Zurwerra, J. Gertsch, K.-H. Altmann, *Org. Lett.* **2010**, *12*, 2302–2305.
- [72] N. Mori, A. Omura, N. Kobayashi, Y. Tsuzuki, *Bull. Chem. Soc. Jpn.* **1965**, *38*, 2149–2155.
- [73] R. Ballini, E. Marcantoni, M. Petrini, *Synth. Commun.* **1991**, *21*, 1075–1081.
- [74] S. N. Mostyn, J. E. Carland, S. Shimmon, R. M. Ryan, R. J. Vandenberg, *ACS Chem. Neurosci.* **2017**, *8*, 1949–1959.
- [75] F. L. Wang, Y. Guo, S. J. Li, Q. X. Guo, J. Shi, Y. M. Li, *Org. Biomol. Chem.* **2015**, *13*, 6286–6290.
- [76] D. L. Boger, R. J. Mathvink, *J. Am. Chem. Soc.* **1990**, *112*, 4008–4011.
- [77] S. Lauzon, F. Tremblay, D. Gagnon, C. Godbout, C. Chabot, C. Mercier-Shanks, S. Perreault, H. DeSève, C. Spino, *J. Org. Chem.* **2008**, *73*, 6239–6250.
- [78] T. M. Brütsch, P. Bucher, K.-H. Altmann, *Chem. Eur. J.* **2016**, *22*, 1292–1300.
- [79] J. F. Díaz, R. Strobe, Y. Engelborghs, A. A. Souto, J. M. Andreu, *J. Biol. Chem.* **2000**, *275*, 26265–26276.
- [80] J. F. Díaz, I. Barasoain, J. M. Andreu, *J. Biol. Chem.* **2003**, *278*, 8407–8419.
- [81] G. M. Sheldrick, *SADABS*, Program for Empirical Absorption Correction of Area Detector Data. Univ. of Göttingen: Göttingen, Germany, **1996**.
- [82] G. M. Sheldrick, *Acta Crystallogr. Sect. A Found. Adv.* **2015**, *71*, 3–8.
- [83] G. M. Sheldrick, *Acta Crystallogr. Sect. A Found. Crystallogr.* **2008**, *64*, 112–122.
- [84] G. M. Sheldrick, *Acta Crystallogr. Sect. C Struct. Chem.* **2015**, *71*, 3–8.
- [85] O. V. Dolomanov, L. J. Bourhis, R. J. Gildea, J. A. K. Howard, H. J. Puschmann, *Appl. Crystallogr.* **2009**, *42*, 339–341.

Manuscript received: March 4, 2023
Accepted manuscript online: April 14, 2023
Version of record online: May 22, 2023